Resolver compatible capacitive rotary position sensor

Fumitaka KIMURA*, Masahiko GONDO†, Akio YAMAMOTO* and Toshiro HIGUCHI*
*Department of Precision Engineering, School of Engineering, The University of Tokyo
7-3-1 Hongo, Bunkyo-ku, Tokyo 113-8656, Japan
Email: {k-bunbun, akio, higuchi}@aml.t.u-tokyo.ac.jp
†SEIDENSHA Co., Ltd.
SIC-2 room 404, 5-4-21 Nishi-Hashimoto, Sagamihara-city, Kanagawa 229-1131, Japan
Email: gondo@seidensha.net

***Abstract*—This paper describes a capacitive rotary position sensor that is characterized by its high compatibility with commercial resolvers. The main components are two electrode plates. Both parts are composed of simple circular or annular electrodes. The sensor is excited by two sinusoidal voltages, which are same as the excitation voltages of resolvers. These excitation voltages are applied to the stator transmitting electrodes. Then, these voltages arise on rotor electrodes by capacitive couplings. The stator pick-up electrodes detect voltages on the rotor that are amplitude-modulated due to the capacitance changes depending on the rotor position. The specifications of these signals are same as those of resolvers. Therefore, the rotor position can be calculated by the same way as resolvers. Due to the similarities with resolvers (excitation signals, generated signals and the way of calculate positions), this sensor can easily replace a commercial resolver. In this paper, the principle is verified by a prototype sensor, which shows a non-linearity error of +/- 4 degrees.**

I. Introduction

Resolvers are widely used as angular position sensors in various positioning applications, due to its robust structure, high reliability for diverse environments and wide acceptable temperature range of operation [1–3]. Typical applications include robots, machine tools and factory automations. Recently, the needs for resolvers have been growing in e.g., automotive applications, such as motor control of hybrid vehicles or electric-powered vehicles due to the increase of crude oil costs and growing awareness of environmental issues. Resolver's structure resembles an electric motor and is essentially a rotary transformer designed so that the coefficient of coupling between rotor and stator windings varies with the shaft angle [4].

Fundamental principles of commercial resolvers are as follows [5–8]. The rotor winding of the resolver is used as primary and is excited by an AC voltage. Here we assume that the input voltage is $e = E\sin\omega t$ where ω is the frequency of excitation voltage and t is time. As a result, the dual-phase windings, which are located in the stator, generate two amplitude-modulated signals

$$e_1 = k\sin\theta\sin\omega t, \tag{1}$$

$$e_2 = k\cos\theta\sin\omega t, \tag{2}$$

where k is a constant determined by the amplitudes of generated signals and θ is the angle of the shaft. The angle of the shaft θ is obtained by calculating

$$\theta = \tan^{-1}(e_1/e_2). \tag{3}$$

This is the basic principle of commercial resolvers.

A resolver is classified into a magnetic-field-based sensor. When a sensor of this type is used in applications of electromagnetic actuator control, a sensor can be affected by magnetic field generated by the actuator. Hence, the resolver requires magnetic shields in order to work correctly. In general, magnetic shielding is realized using magnetic materials, for example, iron [9]. However, magnetic shield becomes thicker and heavier in some heavy applications like electric-powered vehicles. Then, the needs for new angular sensors that are free from the magnetic field interference are increasing.

Such sensors that can replace magnetic-field-based type include optical type and electrostatic capacitive type. Optical sensors mainly consist of a glass scale and a sensor head, which includes a light source and photodiodes. The light source lights up the glass scale and photodiodes detect the reflected light from the glass scale. An optical sensor can measure angular position with a very fine resolution, which is up to nanometer accuracy, if special glass scales are used. However, glasses can break easily, if they are used in heavy applications like vehicles. Therefore, optical sensors cannot easily replace resolvers due to its low durability.

Capacitive rotary position sensors realize low energy consumption, simple structure, high accuracy and resolution [10]. The main components are electrode plates only, which makes the reliability for the environments high enough to replace resolvers. In [11–16], capacitive angular position sensors have been already proposed. However, comparing the existing capacitive angular sensors with resolvers, it can be found that, regardless of their structures, signal specifications are different from conventional resolvers. Therefore, they cannot easily replace resolvers.

This paper proposes a capacitive angular sensor that can easily replace a resolver. To realize highly compatible signals with the commercial resolvers, this sensor is designed to generate signals which specifications are the same as those of commercial resolvers. In addition, the rotor has no cables because the operation of this sensor is based on the capacitive

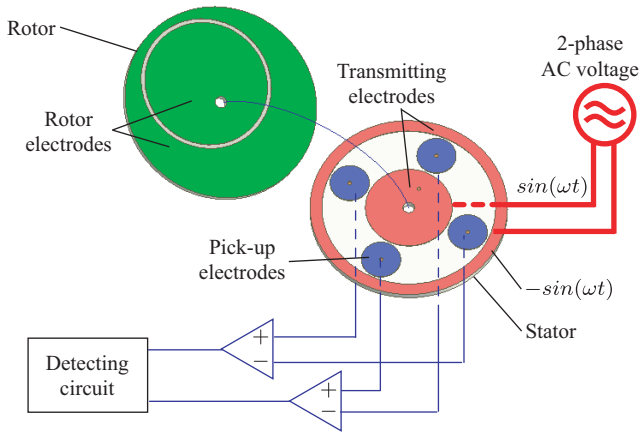

Fig. 1. Schematic diagram of electrostatic capacitive sensor

coupling between the stator and the rotor. Therefore, this sensor does not require slip rings, which is the advantage of this sensor.

In this paper, we propose its analytical model and analyze its working principle. Then, we experimentally verify the performance of the sensor using a prototype sensor system.

II. Basic Principle and Design

A. Structure

Fig. 1 shows the schematic diagram of the capacitive rotary position sensor. It mainly consists of two parts: a stator and a rotor.

The stator has six circular or annular electrodes. Two of the six electrodes, which are on the center and the periphery of the stator plates, are referred to as transmitting electrodes as shown in Fig. 1. The other four electrodes, which have equal radius, are referred to as pick-up electrodes.

The rotor plate is divided by an eccentric circle as shown in Fig. 1. The resulting two electrodes are called rotor electrodes. The rotor has no cables. Thus, slip rings are not needed, unlike resolvers.

B. Principle

As in resolvers, the sensor is excited by two sinusoidal signals with high frequency. These signals are applied to two transmitting electrodes. Then those signals arise on the rotor by capacitive coupling between transmitting and rotor electrodes. In order to keep the same amplitudes of the two signals, the transmitting electrodes and the rotor electrodes are designed to keep the same overlapping area during operation. Then, the signals on the rotor are detected by pick-up electrodes through capacitive coupling between the rotor and the pick-up electrodes. Detected signals are amplitude-modulated depending on the capacitance changes between the rotor and the pick-up electrodes. Therefore, the pick-up electrodes generate amplitude-modulated signals as shown in equations (1) and (2). Eventually, angular position is calculated by equation (3). This is the fundamental principle of this angular position sensor. The operation range is full circle and the resolution depends on the signal processor.

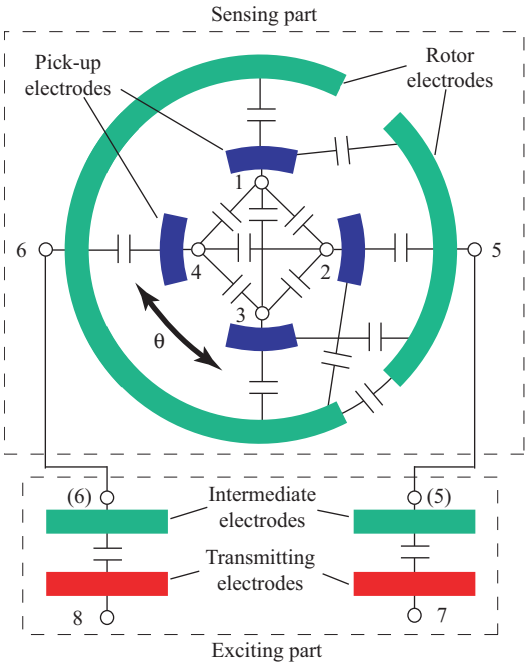

Fig. 2. Equivalent circuit model for analysis

C. Analytical model

Fig. 2 shows an analytical equivalent model using eight terminals for this sensor. In this model, the whole sensor is divided into two parts; the sensing part, which is used as sensing element, and the exciting part, which is used to excite the rotor. In the exciting part, intermediate electrodes and terminals are defined as shown in Fig. 2, for ease of calculation. The terminals 1 through 4 correspond to the pick-up electrodes on the stator, the terminals 5 and 6 correspond to the rotor electrodes, and the terminals 7 and 8 correspond to the transmitting electrodes on the stator. No. 5 and 6 terminals are intermediate terminals.

Among the electric terminals, capacitances are formed between any pair of terminals as shown in Fig. 2. Such capacitances can be mathematically represented using a capacitance coefficient matrix [17]. Considering the geometrical symmetric property among terminals, the matrix for this sensor can be expressed as 8×8 matrix [18], which can be decomposed into two different parts, $\mathbf{C}_{\mathrm{exc}}$ and $\mathbf{C}_{\mathrm{sen}}$. The matrix $\mathbf{C}_{\mathrm{exc}}$, which is the matrix of the exciting part in Fig. 2, is approximated as:

$$\mathbf{C}_{\mathrm{exc}} = \left[\begin{array}{c|cccc} \mathbf{O}_4 & \multicolumn{4}{c} \mathbf{O}_4 \\ \hline \mathbf{O}_4 & \begin{matrix} C_{\mathrm{i}} & 0 & -C_{\mathrm{i}} & 0 \\ 0 & C_{\mathrm{i}} & 0 & -C_{\mathrm{i}} \\ -C_{\mathrm{i}} & 0 & C_{\mathrm{i}} & 0 \\ 0 & -C_{\mathrm{i}} & 0 & C_{\mathrm{i}} \end{matrix} \end{array}\right], \tag{4}$$

where C_{i} is the capacitances between rotor electrodes and

transmitting electrodes. However, some of capacitances between rotor and transmittig electrodes in (4) are approximated as 0. The matrix $\mathbf{C}_{\rm sen}$, which is the matrix of the sensing part in Fig. 2, is represented as:

$$\mathbf{C}_{\rm sen} = \left[\begin{array}{cccc} C_{\rm st} & 0 & \cdots & 0 \\ 0 & C_{\rm st} & \ddots & \vdots \\ \vdots & \ddots & C_{\rm st} & 0 \\ 0 & \cdots & 0 & C_{\rm st} \\ C_{\rm m}(\theta) & C_{\rm m}\left(\theta-\frac{\pi}{2}\right) & C_{\rm m}(\theta-\pi) & C_{\rm m}\left(\theta+\frac{\pi}{2}\right) \\ C_{\rm m}(\theta-\pi) & C_{\rm m}\left(\theta+\frac{\pi}{2}\right) & C_{\rm m}(\theta) & C_{\rm m}\left(\theta-\frac{\pi}{2}\right) \\ \hline \multicolumn{4}{c}{\mathbf{0}_{24}} \end{array}\right.$$

$$\left.\begin{array}{cc|c} C_{\rm m}(\theta) & C_{\rm m}(\theta-\pi) & \\ C_{\rm m}\left(\theta-\frac{\pi}{2}\right) & C_{\rm m}\left(\theta+\frac{\pi}{2}\right) & \\ C_{\rm m}(\theta-\pi) & C_{\rm m}(\theta) & \mathbf{0}_{62} \\ C_{\rm m}\left(\theta+\frac{\pi}{2}\right) & C_{\rm m}\left(\theta-\frac{\pi}{2}\right) & \\ C_{\rm sl} & -C_{\rm l} & \\ -C_{\rm l} & C_{\rm sl} & \\ \hline \multicolumn{2}{c|}{\mathbf{0}_2} & \mathbf{0}_2 \end{array}\right], \quad (5)$$

where

$$C_{\rm m}(\theta) = -C_{\rm m0} - C_{\rm m1}\cos(\theta), \quad (6)$$

$C_{\rm st}$, $C_{\rm sl}$, $C_{\rm l}$, $C_{\rm m0}$ and $C_{\rm m1}$ are all positive constants determined by the geometrical relationship among the terminals. The variable θ is the angular displacement of the rotor.

Among these coefficients, only $C_{\rm m}(\theta)$ is the function of the rotor angular position and is approximated by sinusoidal functions; the other coefficients are simply approximated by constants. In addtion, two kinds of capacitances between pick-up electrodes, and pick-up electrodes and rotor electrodes are approximated as 0. These approximations are based on the operation principle and the electrode design, and will be verified later in the experimental section.

Using the capacitance coefficients matrix, the relationship between charges and the voltages on the terminals can be calculated as:

$$\mathbf{q} = (\mathbf{C}_{\rm exc} + \mathbf{C}_{\rm sen})\mathbf{V}, \quad (7)$$

where $\mathbf{q}$ and $\mathbf{V}$ are 8×1 vectors that represent the charges and the voltages on the eight terminals respectively.

D. Signal analysis

In this section, we analyze the voltages that appear on the pick-up electrodes. In our sensor setup, excitation voltages are applied to the driving electrodes on the stator, which are terminals 7 and 8. Therefore, the voltage vector $\mathbf{V}$ becomes

$$\mathbf{V} = \{V_1, V_2, V_3, V_4, V_5, V_6, V\sin\omega t, -V\sin\omega t\}, \quad (8)$$

where V, and ω are the voltage amplitude and the angular frequency of the applied voltages. Variables V_1 through V_6 are unknown.

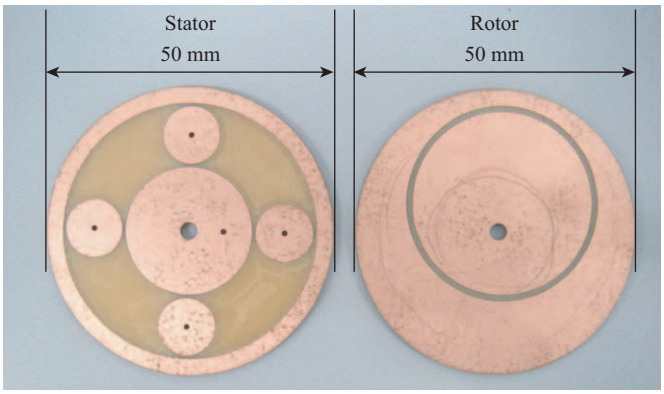

Fig. 3. Photograph of the stator (left) and the rotor (right) plates.

Next, we define the charge vector $\mathbf{q}$ as

$$\mathbf{q} = \{0, 0, 0, 0, 0, 0, q_7, q_8\}, \quad (9)$$

where q_7 and q_8 are the charges given to the transmitting electrodes by the signal source. To determine the charges on the terminals 1 through 4, we introduced an assumption; the voltages of the pick-up electrodes will be measured using high input impedance circuit and thus no electric charge will flow into or out from these electrodes. Due to this assumption, the charges on the terminals 1 through 4 become zero. The charges on the terminals 5 and 6 are also determined as zero, since they are not connecting to any electric power source.

Substituting (4), (5), (8) and (9) into (7) derives the induced voltages V_1, V_2, V_3, and V_4 as:

$$\left\{\begin{array}{l} V_1 = \quad K_c V\cos(\theta)\sin(\omega t) \\ V_2 = \quad K_c V\sin(\theta)\sin(\omega t) \\ V_3 = -K_c V\cos(\theta)\sin(\omega t) \\ V_4 = -K_c V\sin(\theta)\sin(\omega t) \end{array}\right., \quad (10)$$

where K_c is

$$K_c = \frac{2C_{\rm i}C_{\rm m1}}{-4{C_{\rm m1}}^2 + C_{\rm st}(C_{\rm i} + C_{\rm l} + C_{\rm sl})}.$$

Equation (10) indicates that the specifications of these signals, which are the voltages on the pick-up electrodes, are amplitude modulated signals that are the same as the signal specification of the resolver as shown in equation (1) and (2). The applied voltages on the driving electrodes are the carrier wave and the rotor position $\sin\theta/\cos\theta$ represents the signal envelope curve. Thus, demodulating these signals will deliver the rotor position θ, which is the basic operation principle of this sensor.

III. Fabrication of a Prototype

A. Electrode plates

The rotor and stator plates of the prototype system are shown in Fig. 3. Both of them are fabricated by copper-clad-laminate. The diameter of both plates is 50 mm.

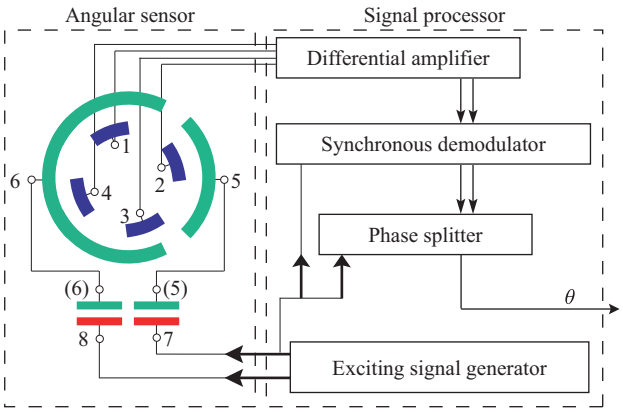

Fig. 4. Electronic interface for the capacitive sensor.

B. Electric circuit and signal processing

Fig. 4 shows the electric interface developed for this prototype sensor. Processes of this interface basically correspond to those of resolvers. The interface consists of differential amplifiers, synchronous demodulators, a phase splitter, and a signal generator.

First, voltages on the pick-up electrodes (10) are measured and amplified by the differential amplifiers as:

$$V_{\mathrm{A}} = K_o(V_1 - V_3) = 2K_oK_c\cos(\theta)\sin(\omega t) \tag{11}$$

$$V_{\mathrm{B}} = K_o(V_2 - V_4) = 2K_oK_c\sin(\theta)\sin(\omega t) \tag{12}$$

where K_o is the amplification ratio of the differential amplifiers. Then, these signals, (11) and (12), are demodulated by the synchronous demodulators, which gives:

$$V_{\mathrm{A}} = A\cos(\theta) \tag{13}$$

$$V_{\mathrm{B}} = A\sin(\theta) \tag{14}$$

where A is the eventual amplification constant after (11) and (12) are multiplied and filtered by the synchronous demodulator. Finally, the phase splitter calculates the phase θ from the signals, (13) and (14).

In this particular prototype, the calculated θ was converted into A/B pulses and counted on a pulse counter. The phase splitter employed in the system generates 1024 pulses per a cycle, which results in a pulse resolution of 0.35 degree.

IV. Experiments

Fig. 5 shows the experimental setup used to test the static characteristics of the prototype sensor. The setup consists of a rotational stage, a tilting stage, and a precision motion stage. The precision motion and tilting stages were used to correctly align the rotor with the stator. The rotational stage was used to give angular displacement to the rotor manually. The angular position of the rotor was measured by the rotational stage.

In this setup, the rotor was wired to verify the principle and the matrices. We also fabricated the sensor with non-wired rotor, which is described in a later section IV-C.

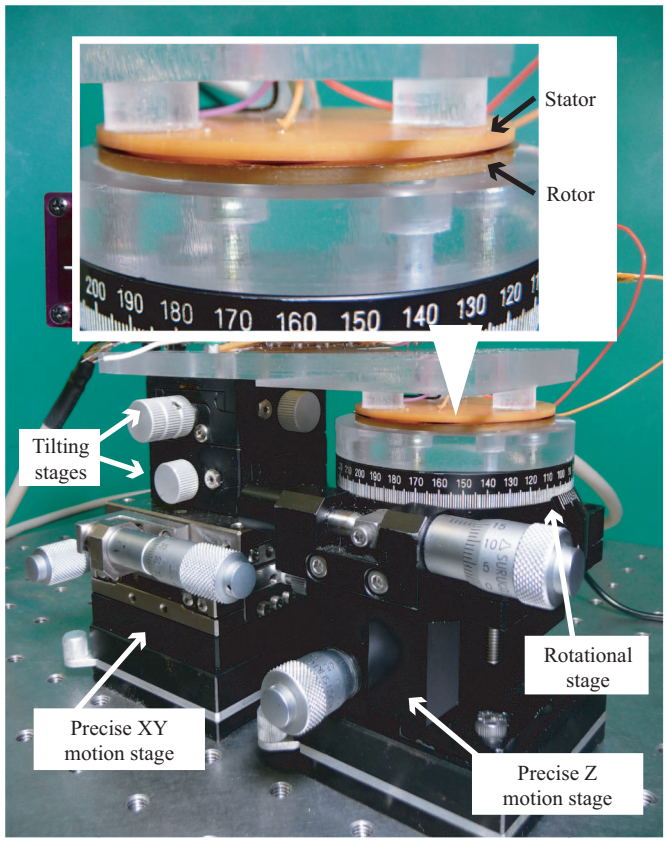

Fig. 5. Experimental setup composed of the capacitive sensor and the rotational stage. The sensor, which is used in this setup, has a wired rotor

A. Capacitances

The capacitance coefficients of (5) were measured using an impedance analyzer as described in [17]. Fig. 6 shows a part of the measurement results of the capacitance coefficients.

Not all the results are shown in the plot due to the limited space. In Fig. 6 (a), capacitance coefficients between the rotor electrodes and the pick-up electrodes are shown. They should change as sinusoidal waves as in (5). However, a part of them form non-sinusoidal wave. This was probably caused by the structure of the electrodes, especially wiring to the rotor. In Fig. 6 (b), capacitance coefficients that should be zero in the matrices (4) and (5) are shown. Most of them can be approximated by 0 as shown in (5). However, C_{58} and C_{67} are not ignorable. This would be due to the design of the electrodes; the proximity of electrodes (C_{58} and C_{67}) should have been avoided.

B. Signals

The measured voltages corresponding to (11) and (12) are plotted in Fig. 7. The excitation voltage applied to the transmitting electrodes had 3.6 V_{p-p} and 20 kHz. The experimental results show amplitude-modulated signals as shown in equations (11) and (12). The envelopes of the two signals have 90 degrees phase shift.

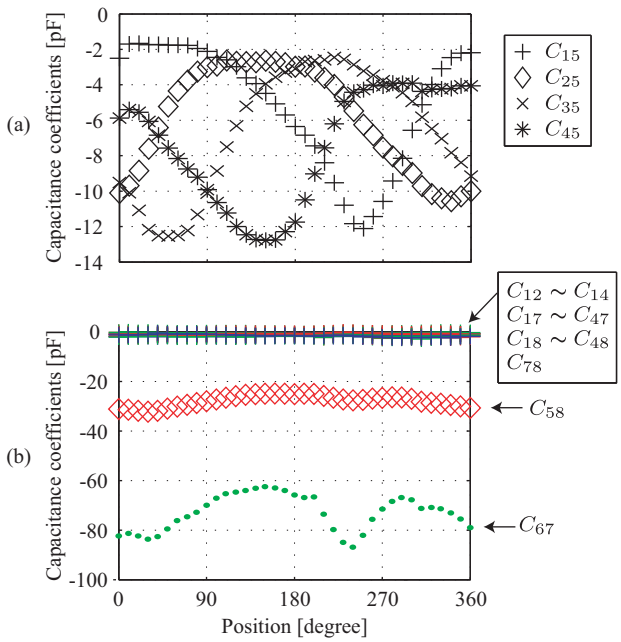

Fig. 6. Measurement results of capacitance coefficients.

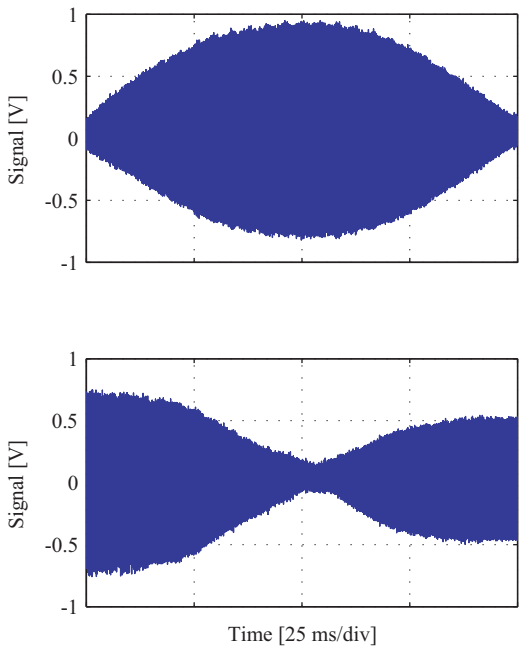

Fig. 7. The measured voltages corresponding to (11) and (12).

C. Linearity

Fig. 8 (a) shows the output of the prototype sensor, which was plotted against the scale of the rotational stage. For this measurement, the rotor rotated one revolution with a step of 10 degrees. Fig. 8 (b) shows the non-linearity error of Fig. 8 (a). From this plot, the maximum non-linearity error of $\pm$ 8 degrees can be found. This error was probably caused by four reasons. The first possible reason is the misalignment

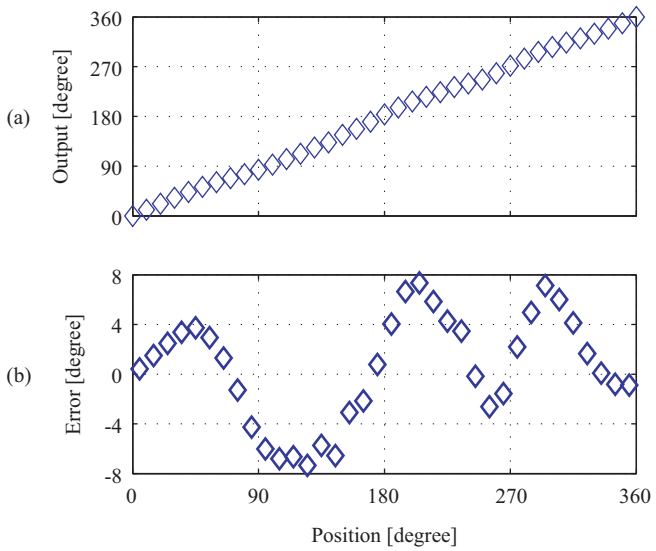

Fig. 8. (A): Output of the rotary popsition sensor, which is shown in Fig. 5, against the position of the rotational stage. (B): Non-linearity error of the prototype.

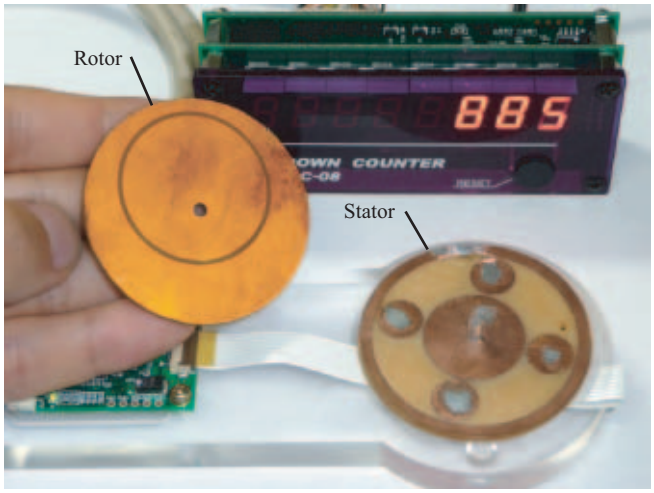

Fig. 9. Another prototype rotary position sensor using non-wired rotor

between the rotor and the stator in the experimental setup. The second is the deviations of the capacitance coefficients between the theoretical ones and the real values, which could be improved by modifying the electrode shapes. The third is interference by stray capacitors, which are formed between cables. They can be reduced by rearranging cables. The last reason is that soldering on electrodes. In this prototype, wires are soldered from behind of electrodes using a through-hole. Resultantly, the surfaces of the electrodes were rough.

As shown in Fig. 9, we also fabricated another prototype sensor which has no cables for rotor. The absence of the rotor wires can reduce the stray capacitances of wires. In addition, the surfaces of the rotor electrodes are flat since they do not need through-holes. The linearity and non-linearity error of this prototype sensor are shown as Fig. 10. As can be

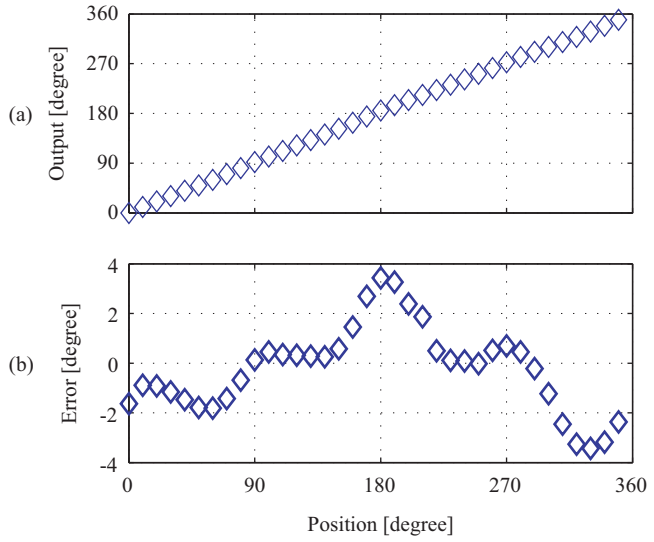

Fig. 10. (A): Output of the rotary popsition sensor which is shown in Fig. 9, against the position of the rotational stage. (B): Non-linearity error of another prototype.

seen in this figure, the non-linearity error is improved in half ($\pm$ 4 degrees) of Fig. 8. Although this sensor has no wire on its rotor, those of its stator are still connected by through-holes. By changing the way of wiring, the error would be improved additionally.

V. Conclusion

This paper proposed a new resolver compatible rotary position sensor. The sensor consists of the rotor and the stator electrode plates. Transmitting electrodes on the stator are energized by two sinusoidal signals. Applied signals are detected by pick-up electrodes through capacitance couplings between the stator and the rotor. Generated signals are amplitude modulated by capacitance change between the stator and the rotor. Its specifications are same as those of resolvers, which realize high compatibility with resolver. In addition, the rotor of this sensor needs no cabling. Slip rings are not needed, unlike commercial resolvers. Based on the capacitance network model, the operation principle was discussed. The operation was experimentally verified using a fabricated prototype. The experimental results showed the maximum non-linearity error of ± 4 degrees.

Acknowledgment

One of the authors (F.K) was supported through the Global COE Program, "Global Center of Excellence for Mechanical Systems Innovation," by the Ministry of Education, Culture, Sports, Science and Technology.

References

[1] M. Katakura, A. Toda, Y. Takagi, N. Suzuki, T. Kadoyama, and H. Kushihara, "A 12-bits resolver-to-digital converter using complex twin pll for accurate mechanical angle measurement," vol. 2005, Kyoto, Japan, 2005, pp. 236 – 239.

[2] K. Masaki, K. Kitazawa, H. Mimura, M. Nirei, K. Tsuchimichi, H. Wakiwaka, and H. Yamada, "Magnetic field analysis of a resolver with a skewed and eccentric rotor," *Sensors and Actuators, A: Physical*, vol. 81, no. 1, pp. 297 – 300, 2000.

[3] M. Benammar, L. Ben-Brahim, and M. Alhamadi, "A novel resolver to 360 degrees; linearized converter," *IEEE Sensors Journal*, vol. 4, no. 1, pp. 96 – 101, 2004/02/.

[4] G. S. Boyes., *Synchro and resolver conversion*. Analog Devices, 1980.

[5] D. Hanselman, "Techniques for improving resolver-to-digital conversion accuracy," *IEEE Transactions on Industrial Electronics*, vol. 38, no. 6, pp. 501 – 4, 1991/12/.

[6] ——, "Resolver signal requirements for high accuracy resolver-to-digital conversion," *IEEE Transactions on Industrial Electronics*, vol. 37, no. 6, pp. 556 – 61, 1990/12/.

[7] G. Woolvet, "Digital transducers," *Journal of Physics E (Scientific Instruments)*, vol. 15, no. 12, pp. 1271 – 80, 1982/12/.

[8] C.-H. Yim, I.-J. Ha, and M.-S. Ko, "A resolver-to-digital conversion method for fast tracking," *IEEE Transactions on Industrial Electronics*, vol. 39, no. 5, pp. 369 – 78, 1992/10/.

[9] M. Fujikura, K. Segawa, K. Chikuma, K. Fujisaki, J. Mino, T. Morita, T. Saito, H. Hirano, and T. Shinnoh, "Open-type magnetic shield structure and its performance," *IEEE Transactions on Magnetics*, vol. 44, no. 11, pp. 4179 – 82, 2008/11/.

[10] L. K. Baxter, *Capacitive Sensors*. IEEE Press, New York, 1997.

[11] R. Peters, "Linear rotary differential capacitance transducer," *Review of Scientific Instruments*, vol. 60, no. 8, pp. 2789 – 93, 1989/08/.

[12] R. Wolffenbuttel and R. Van Kampen, "An integrable capacitive angular displacement sensor with improved linearity," vol. A27, no. 1-3, Switzerland, 1991/05/, pp. 835 – 43.

[13] G. de Jong, G. Meijer, K. van der Lingen, J. Spronck, A. Aalsma, and T. Bertels, "A smart capacitive absolute angular-position sensor," vol. A41, no. 1-3, Switzerland, 1994/04/01, pp. 212 – 16.

[14] X. Li, G. Meijer, G. de Jong, and J. Spronck, "An accurate low-cost capacitive absolute angular-position sensor with a full-circle range," vol. 45, no. 2, USA, 1996/04/, pp. 516 – 20.

[15] G. Brasseur, P. Fulmek, and W. Smetana, "Virtual rotor grounding of capacitive angular position sensors," *IEEE Transactions on Instrumentation and Measurement*, vol. 49, no. 5, pp. 1108 – 11, 2000/10/.

[16] M. Gasulla, X. Li, G. Meijer, L. van der Ham, and J. Spronck, "A contactless capacitive angular-position sensor," *IEEE Sensors Journal*, vol. 3, no. 5, pp. 607 – 14, 2003/10/.

[17] A. Yamamoto, T. Niino, and T. Higuchi, "Modeling and identification of an electrostatic motor," *Precision Engineering*, vol. 30, no. 1, pp. 104–13, Jan. 2006.

[18] N. Yamashita, Z. G. Zhang, A. Yamamoto, M. Gondo, and T. Higuchi, "Voltage-induction type electrostatic film motor driven by two- to four-phase ac voltage and electrostatic induction," *Sensors and Actuators, A: Physical*, vol. 140, no. 2, pp. 239 – 250, 2007, electrostatic induction;Electrostatic motor;Film actuator;Flexible printed circuit;Synchronous motor;. [Online]. Available: http://dx.doi.org/10.1016/j.sna.2007.07.007